Organic geochemistry and paleoenvironmental reconstruction

Jörn Peckmann

AG Geologie im Erdsystem
Institut für Geologie
Universität Hamburg
DER FORSCHUNG | DER LEHRE | DER BILDUNG

Hypersaline pond, Sicily

SaltGiant Short Course 1

Modern and ancient oceans

Salamaca, November 25

Universidad de Salamanca
Campus de Excelencia Internacional

MedSalt

SaltGiant

Universität Hamburg

cen

Organic geochemistry and paleoenvironmental reconstruction

(1) Lipid biomarkers – an introduction

(2) Biomarker proxies for paleoenvironment reconstruction

(3) Deeper-water sections of the Tertiary Piedmont Basin

(4) Primary gypsum with filamentous microfossils

(5) Calcare di Base, Sicily and Calabria

Lipid biomarkers – an introduction

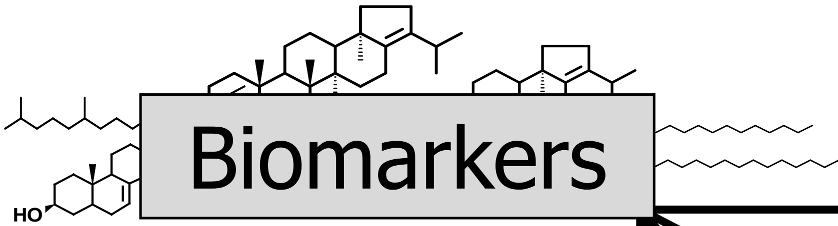

Biomarkers

- Lipids
  (e.g. cell membrane constituents)
- <1000 amu
- persistent carbon skeletons

Chemotaxonomy

Biocommunities

Environment

Biogeochemical processes

Maturity (P,T)
Oil corellation

The tree of life

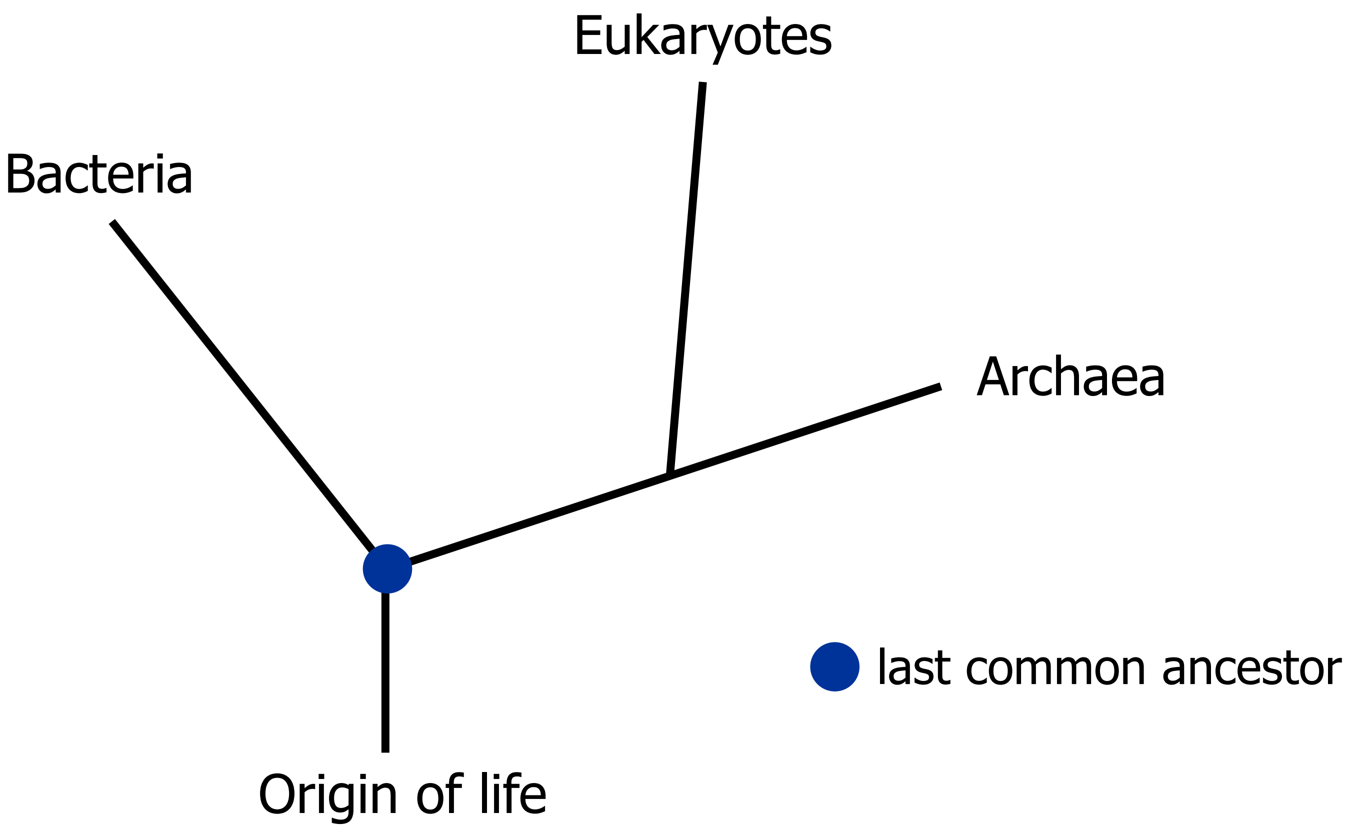

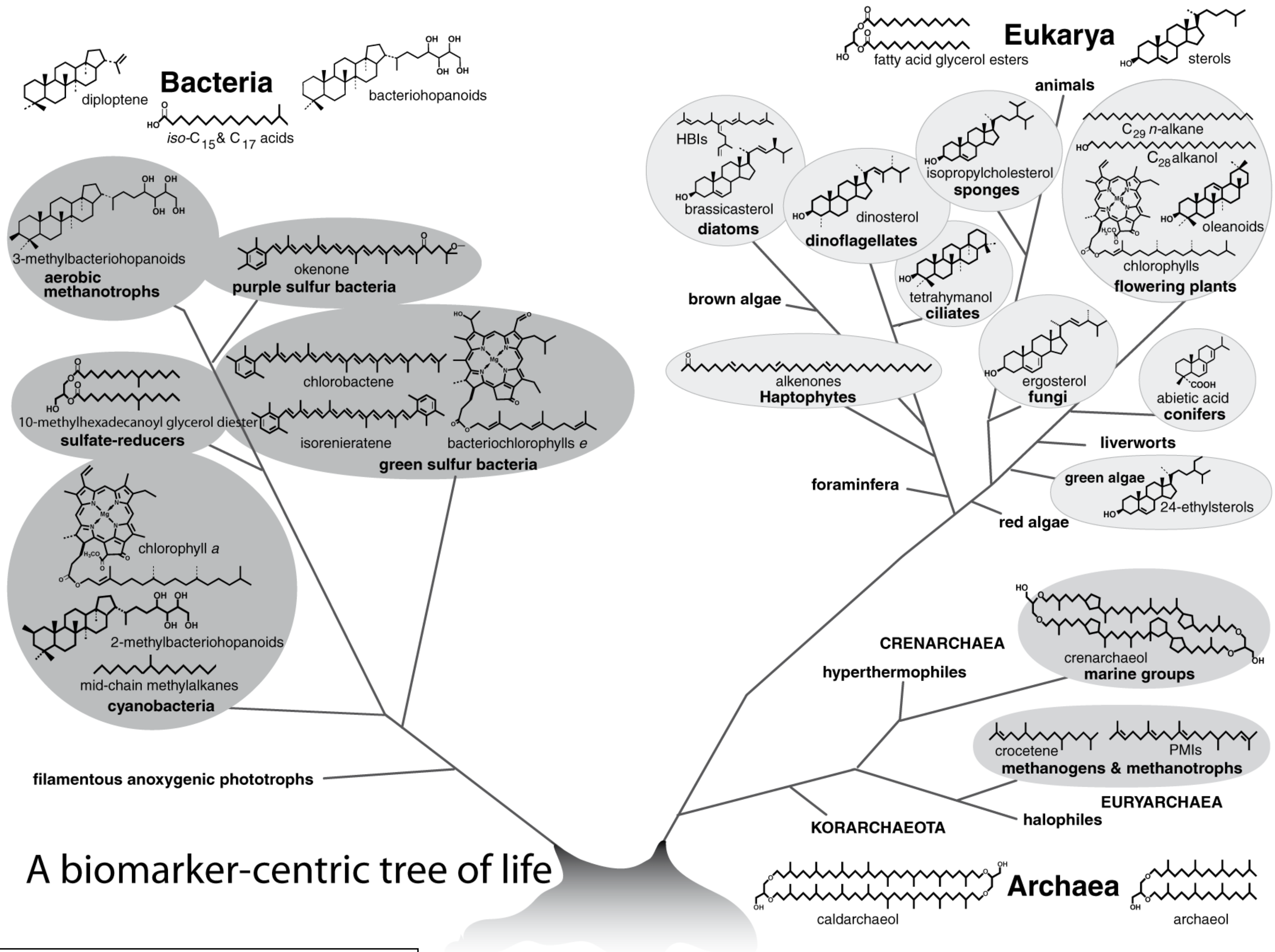

A biomarker-centric tree of life

Echoes of Life – Gaines et al. 2009

The biomarker concept

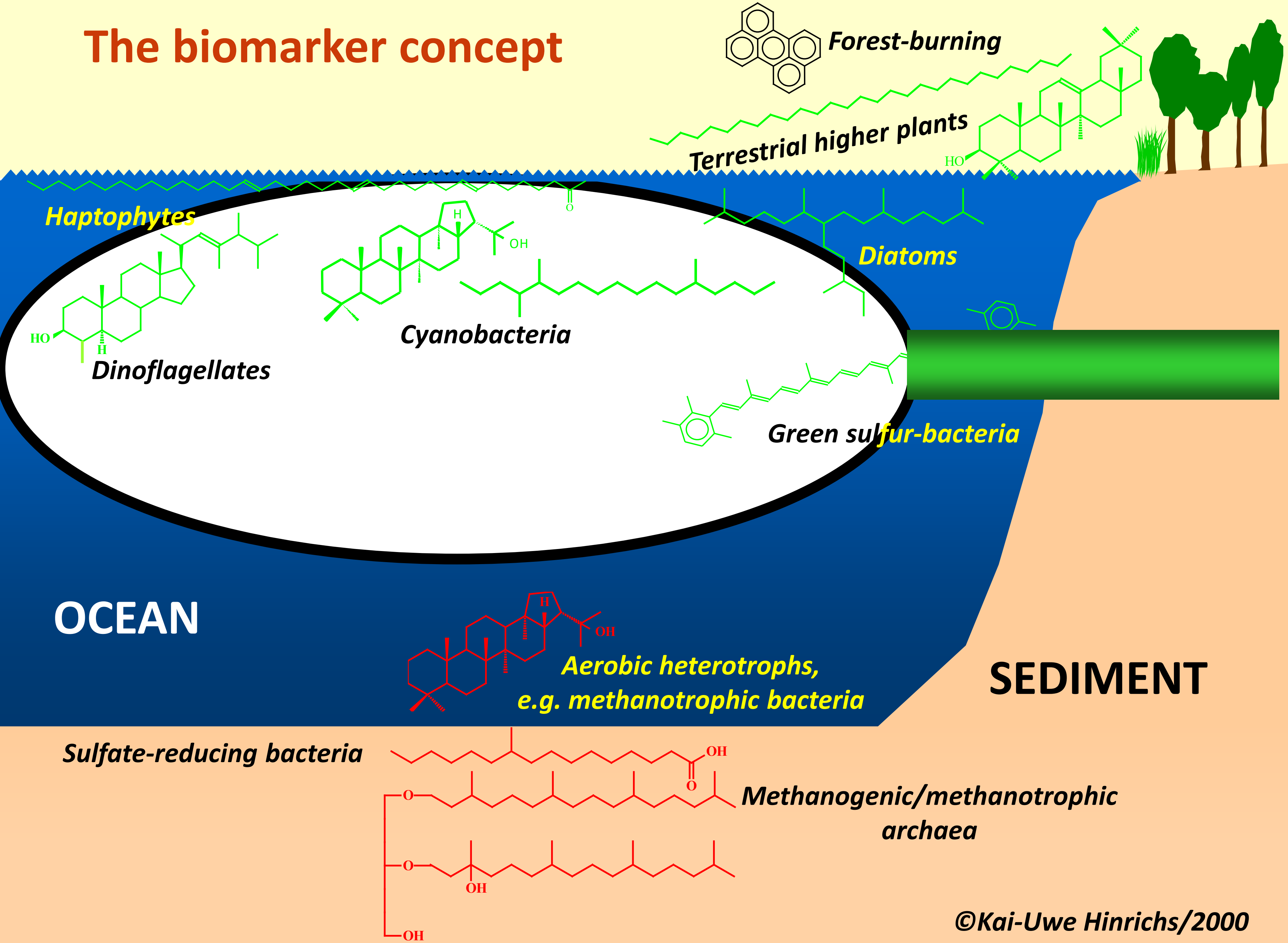

The biomarker concept

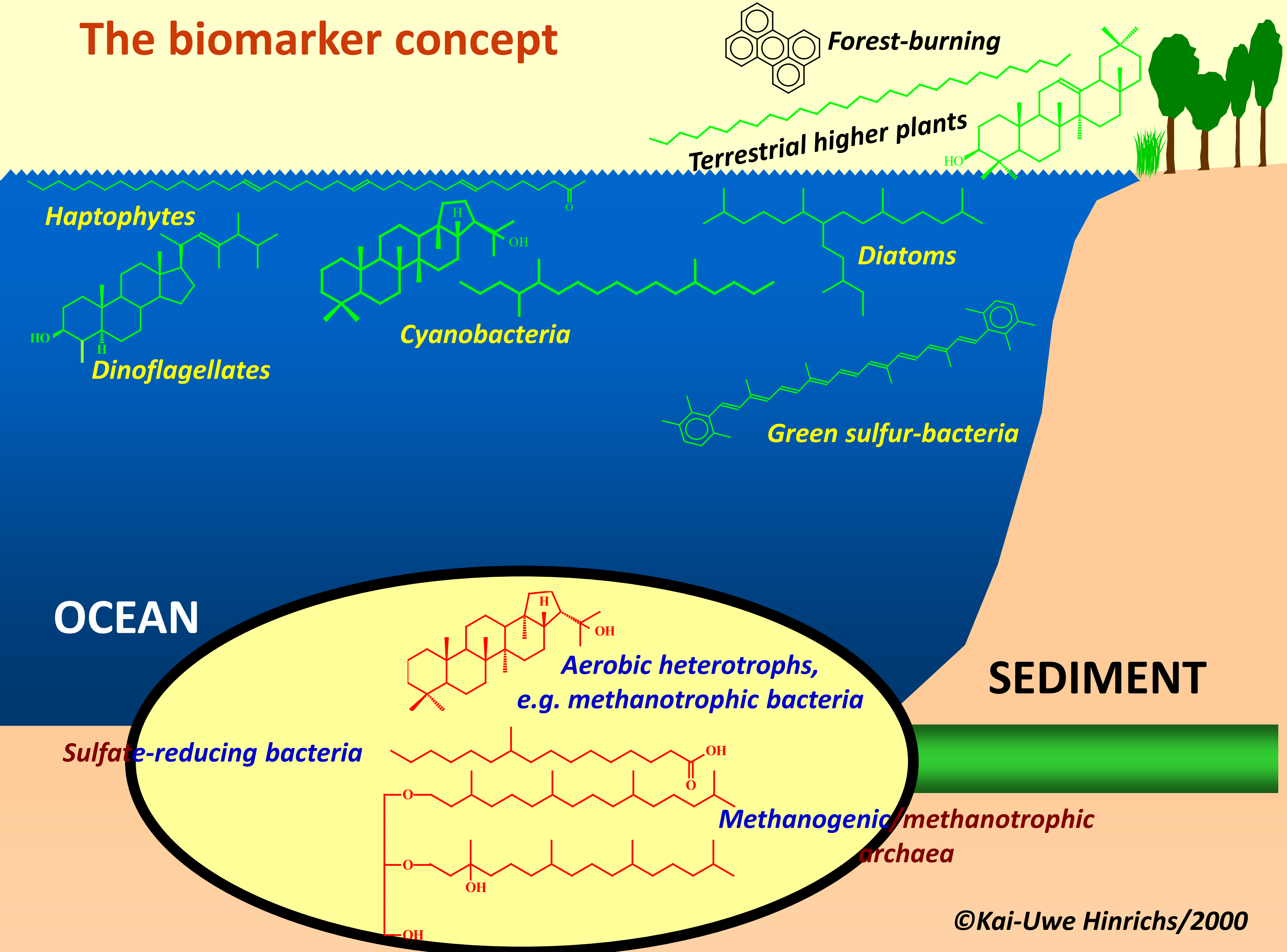

Archaeal lipids

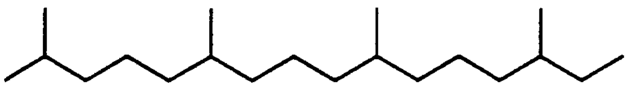

2,6,10,14-tetramethylhexadecane (phytane)

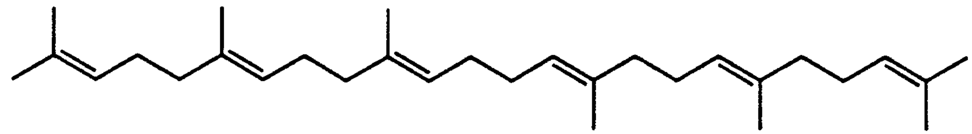

2,6,10,15,19,23-hexamethylhexacos-2,6,10,14,18,22-hexaene (squalene)

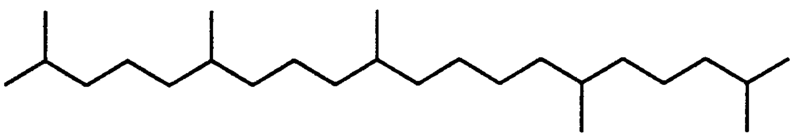

2,6,10,15,19-pentamethyleicosane (PME) → PMI

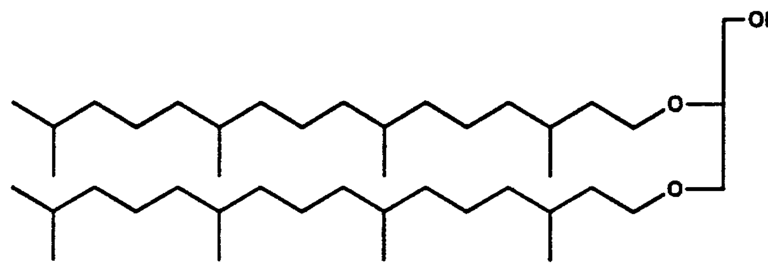

2,3-di-*O*-phytanyl-*sn*-glycerol (archaeol)

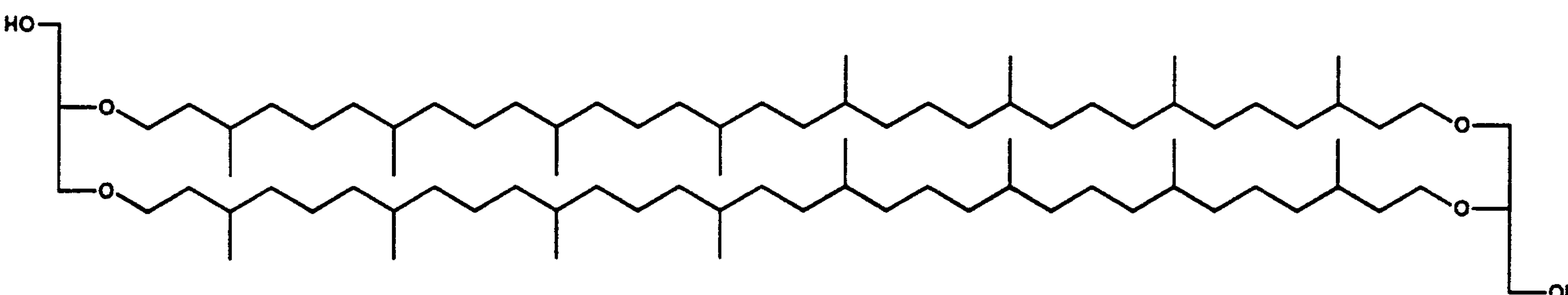

2,3-di-*O*-biphytanyl-*sn*-diglycerol (caldarchaeol)

GDGT = glycerol dialkyl (**dibiphytanyl**) glycerol tetraether

Biomarker proxies for paleoenvironment reconstruction

Sediments: 82% of carbon are fived as carbonate, only 18% are C_{org}

! approx. 0.01% of carbon fixed in primary production enters the geological carbon cycle !

3 $x10^{12}$t C_{org}

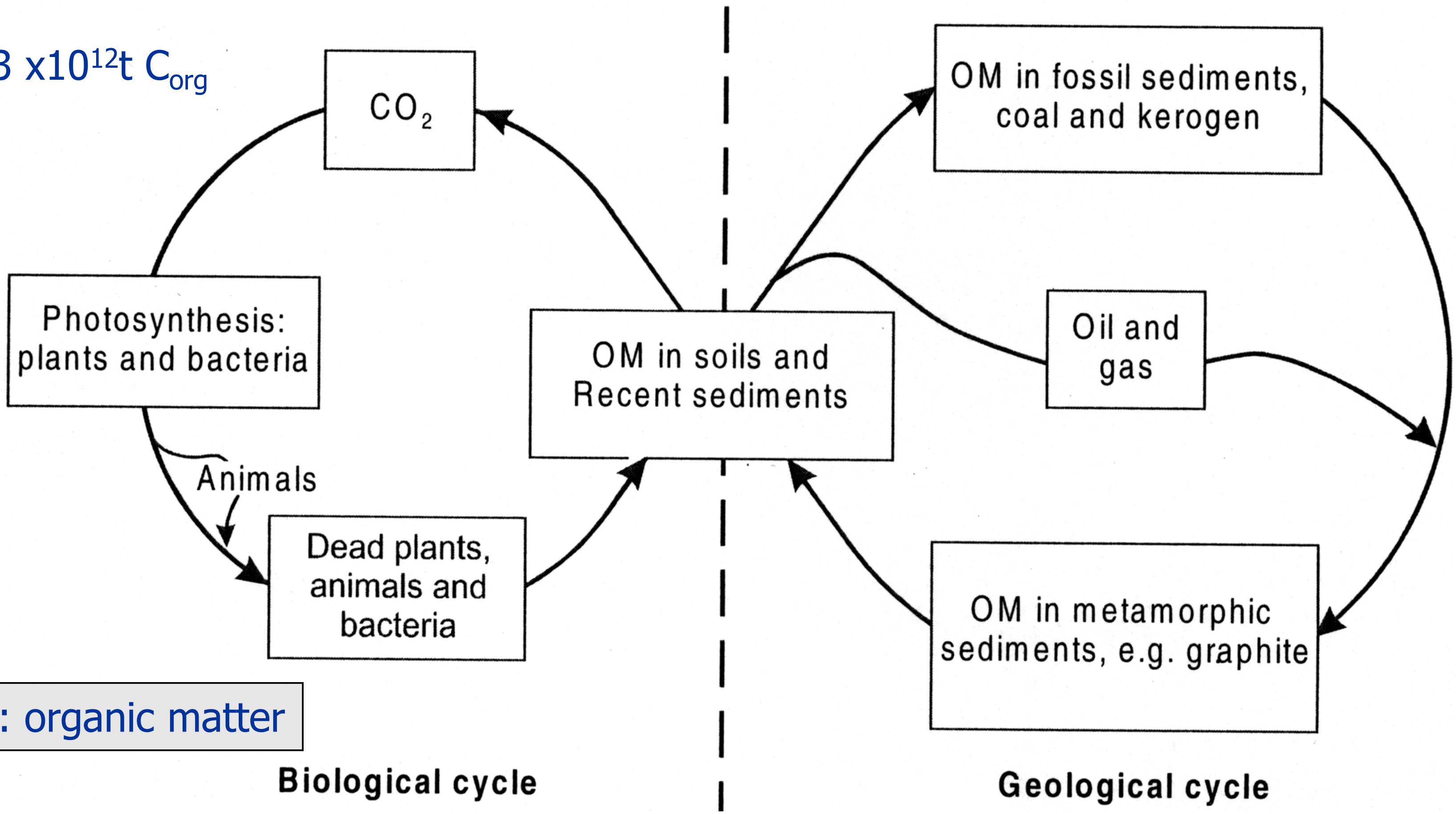

OM: organic matter

6.4 x 10^{15} t C_{org}

Rullkötter 2000

The fate of organic matter

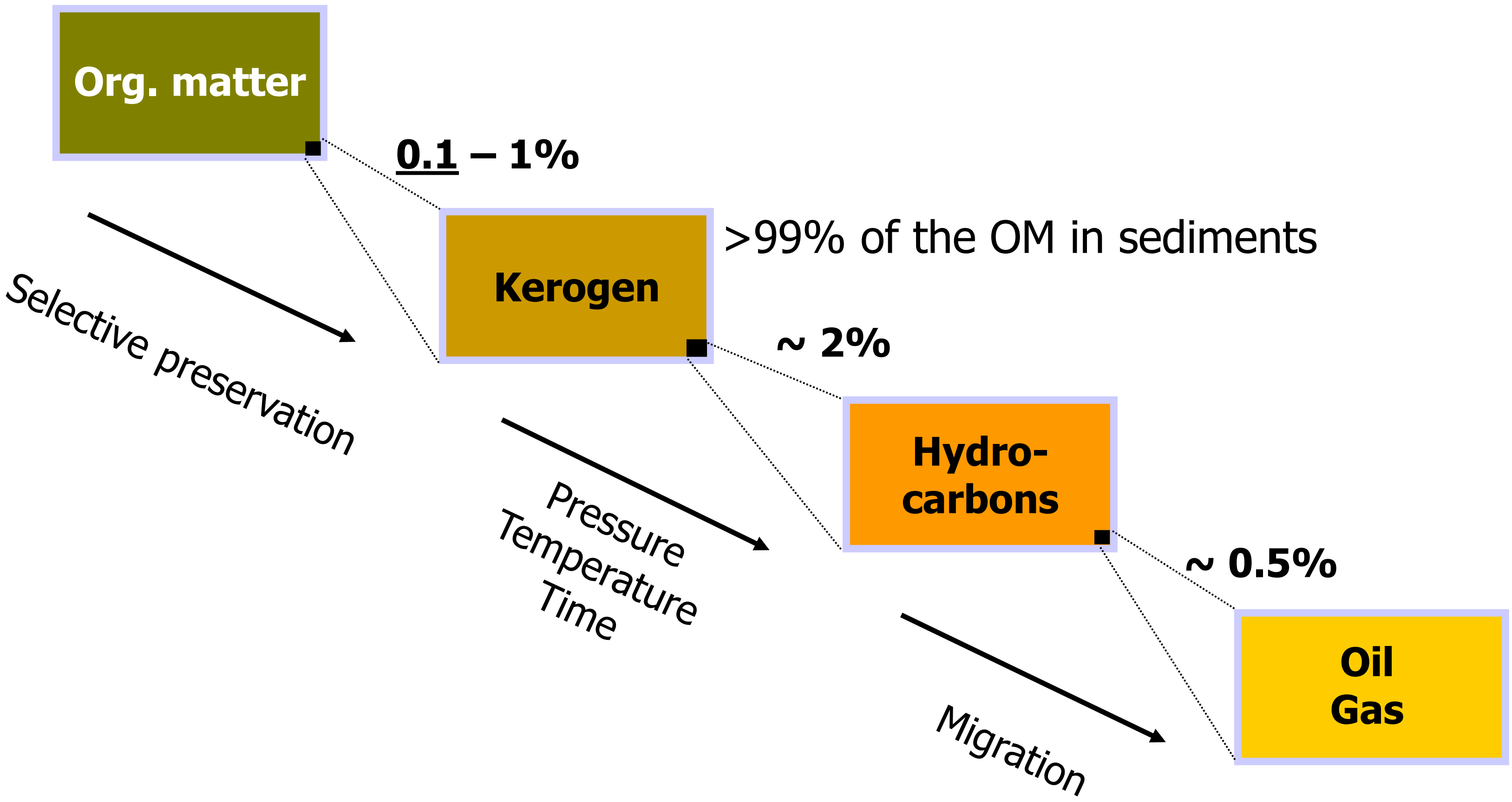

Universität Hamburg

cen

Pristane/phytane ratios as an indicator of redox conditions

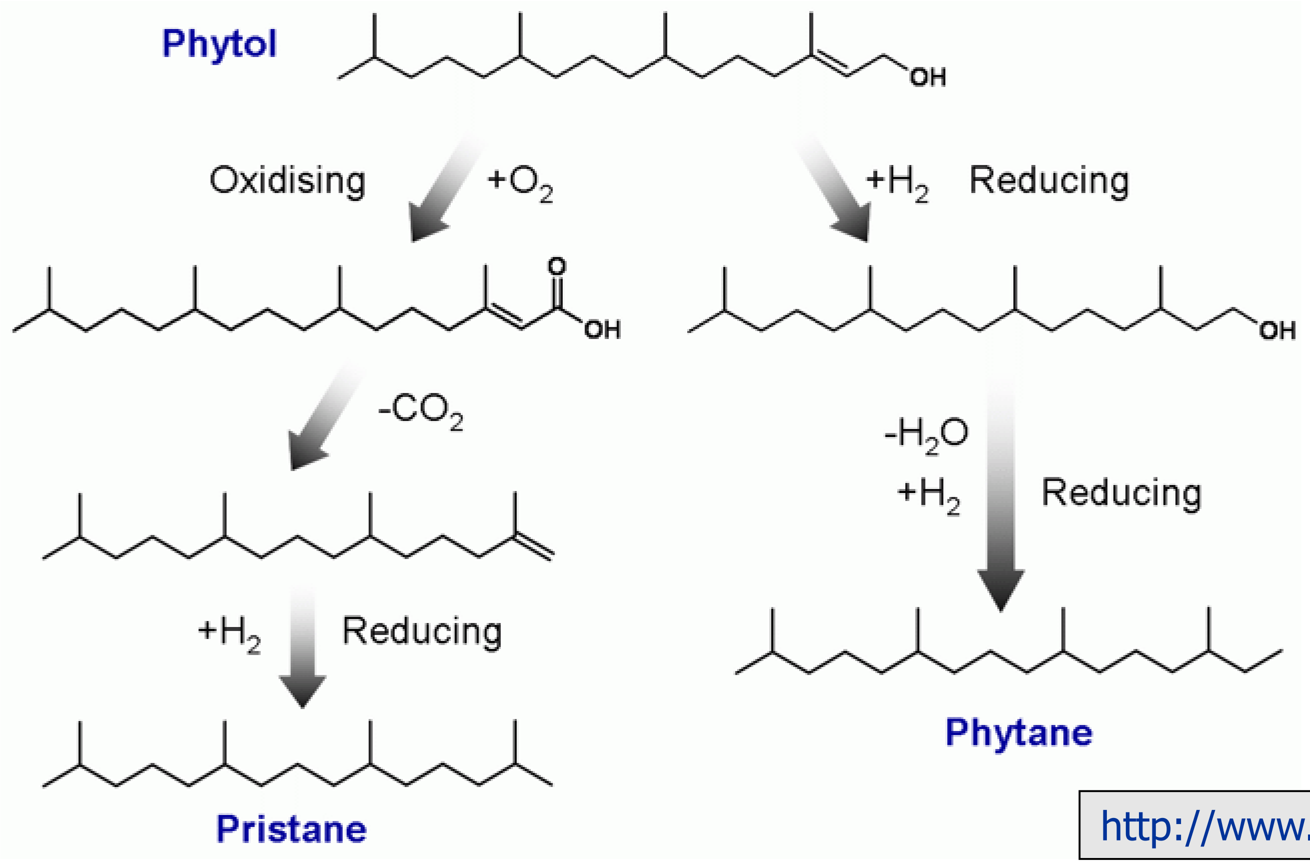

http://www.igiltd.com/

pristane/phytane ratios of >1 indicate oxic conditions during sedimentation (at the sediment/water interface), whilst values of <1 reflect anoxic conditions

Terrestrial/aquatic ratios (TAR)

TAR for hydrocarbons: $(\textit{n}\text{-}C_{27} + \textit{n}\text{-}C_{29} + \textit{n}\text{-}C_{31}) / (\textit{n}\text{-}C_{15} + \textit{n}\text{-}C_{17} + \textit{n}\text{-}C_{19})$

TAR for fatty acids: $(\textit{n}\text{-}C_{24} + \textit{n}\text{-}C_{26} + \textit{n}\text{-}C_{28}) / (\textit{n}\text{-}C_{12} + \textit{n}\text{-}C_{14} + \textit{n}\text{-}C_{16})$

Bourbonniere and Meyers 1996

Carbon Preference Index (CPI)

$$\mathrm{CPI} = 0.5 \times \left(\frac{C_{25} + C_{27} + C_{29} + C_{31} + C_{33}}{C_{24} + C_{26} + C_{28} + C_{30} + C_{32}} + \frac{C_{25} + C_{27} + C_{29} + C_{31} + C_{33}}{C_{26} + C_{28} + C_{30} + C_{32} + C_{34}} \right)$$

Bray and Evans 1961

Represents the predominance of odd over even *n*-alkanes → measure of the freshness of terrestrial organic matter

Average Chain Length index (ACL index)

$$ACL = \frac{25 \times C_{25} + 27 \times C_{27} + 29 \times C_{29} + 31 \times C_{31} + 33 \times C_{33}}{C_{25} + C_{27} + C_{29} + C_{31} + C_{33}}$$

Poynter and Eglinton 1990

traces changes in the sources of higher plant-derived *n*-alkanes; C_3 plants tend to produce shorter *n*-alkane chains

Archaeol Caldarchaeol Ecometric (ACE)

ACE = [archaeol / (archaeol + caldarchaeol)] x 100

Caldarchaeol = GDGT-0

Salinity = (ACE + 9.7) / 0.38

Turich and Freemann 2011

Universität Hamburg

cen

Branched Isoprenoid Tetraether (BIT) index

BIT = (I + II + III) / (I + II + III + crenarchaeol)

I, II, and III refer to the branched GDGTs with m/z 1022, 1036, and 1050

Hopmans et al. 2004

based on the relative abundance of terrigenous branched non-isoprenoidal

tetraethers versus marine-derived crenarchaeol

Deeper-water sections of the Tertiary Piedmont Basin

The Pollenzo section

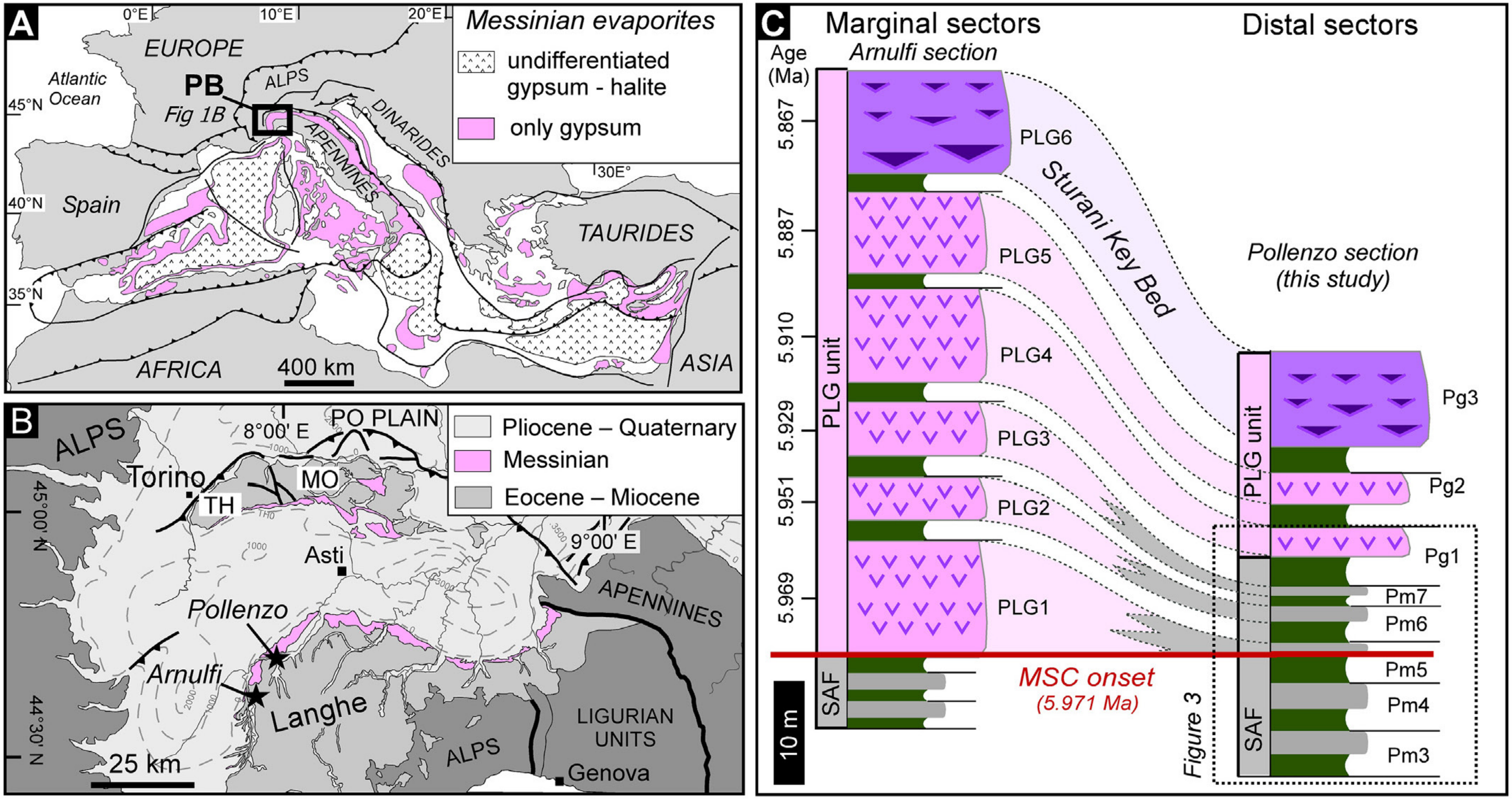

Natalicchio et al. 2019

An archive of environmental change in the absence of evaporites

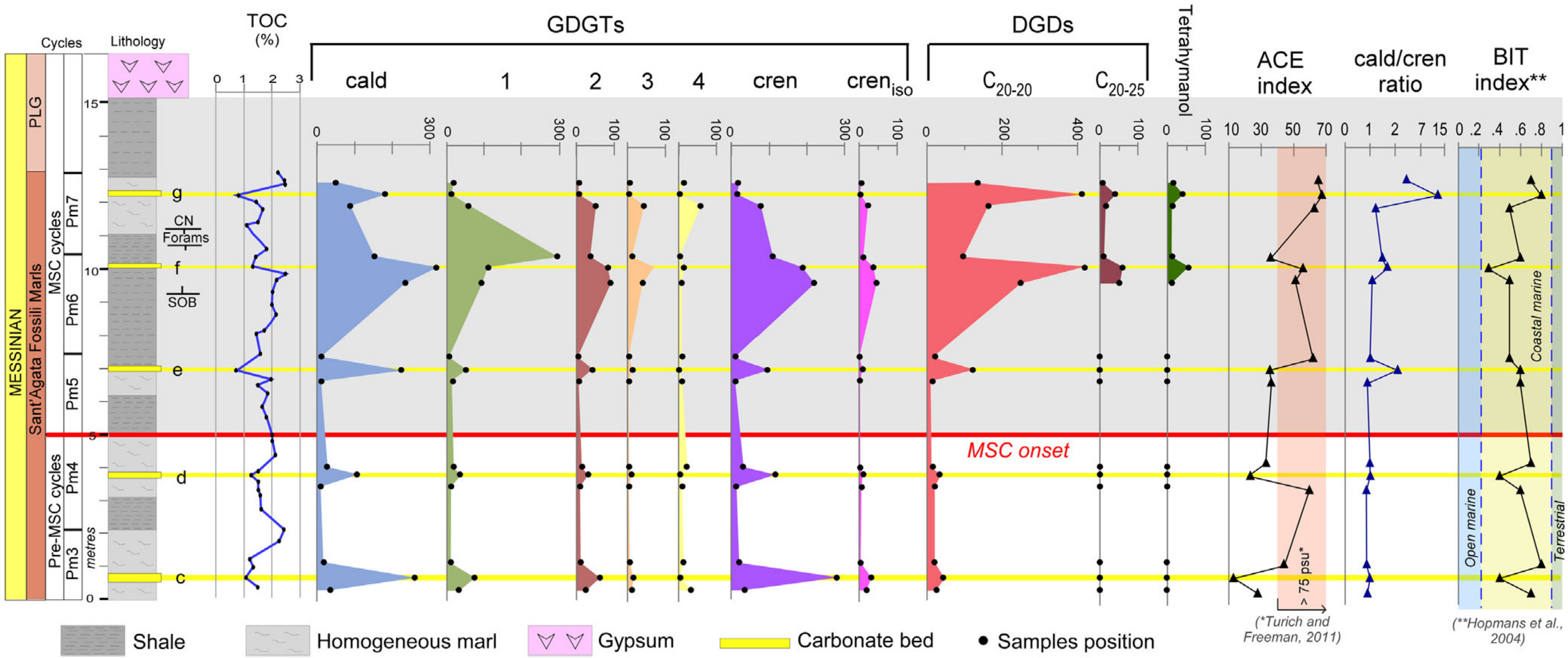

Natalicchio et al. 2017

A precession-paced succession

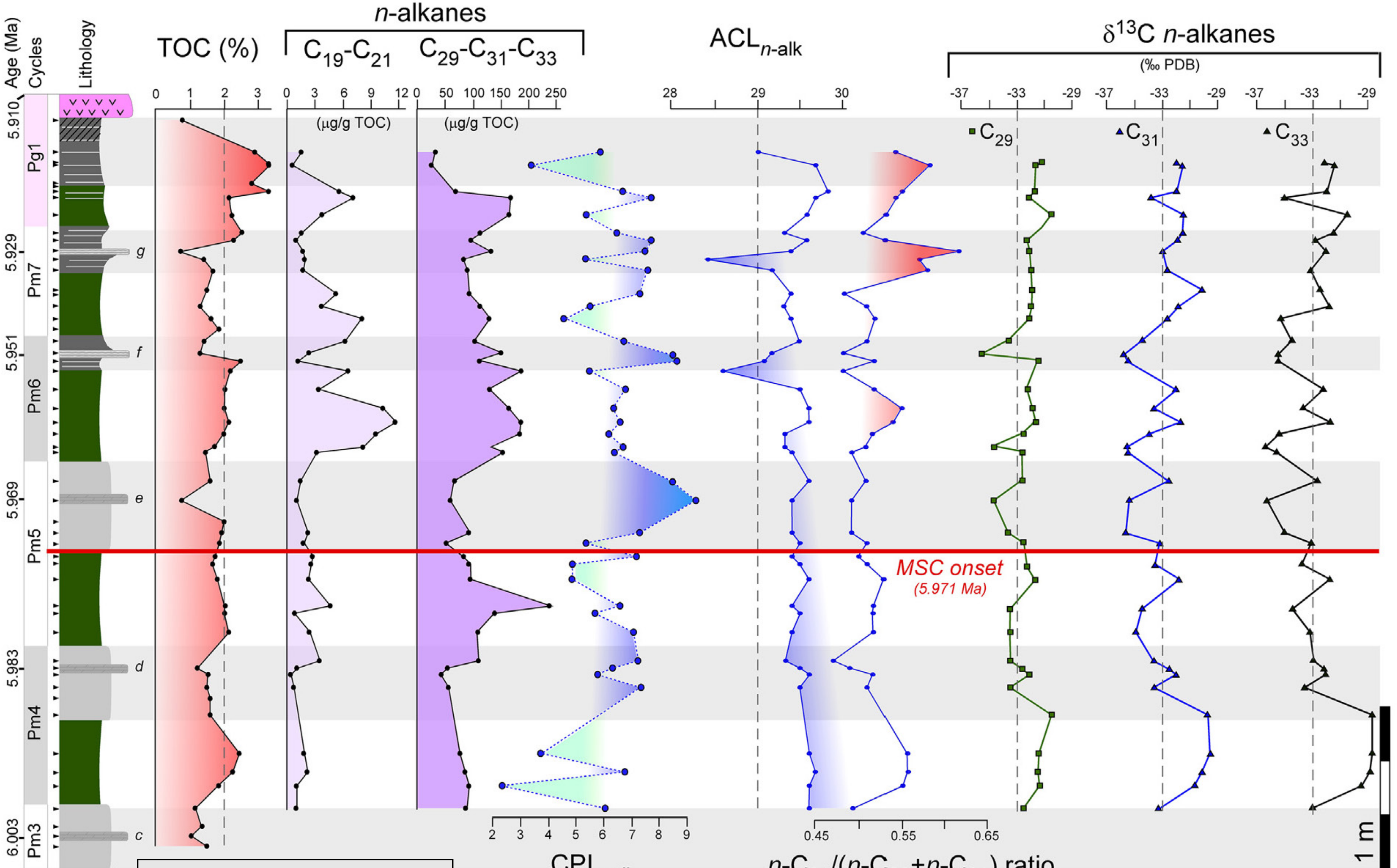

Natalicchio et al. 2019

A precession-paced succession

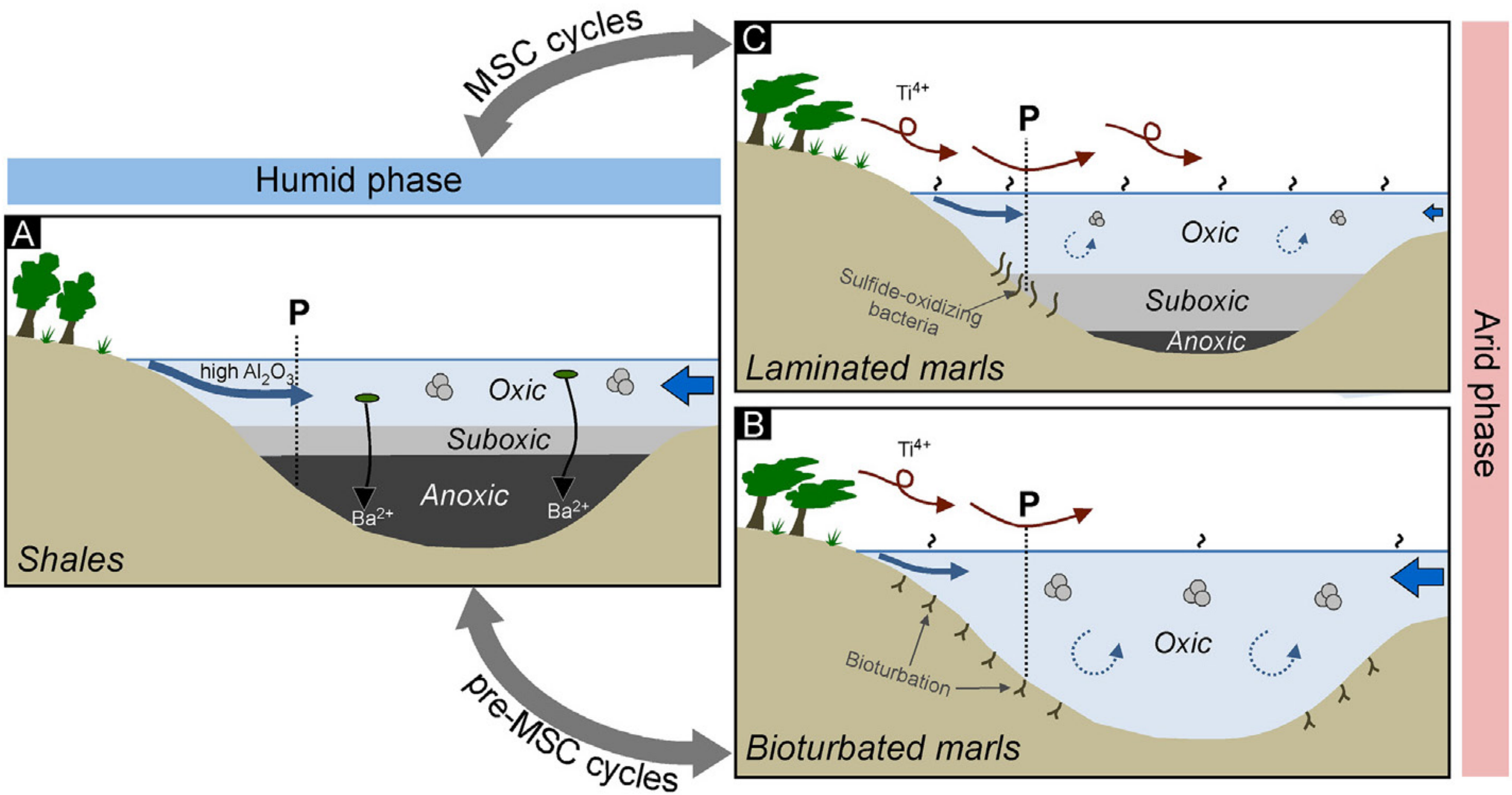

Natalicchio et al. 2019

Conclusions – Piedmont basin

1. Archaea dominated in the water column and sediments after the onset of the Messinian salinity crisis

2. Shales deposited during humid phases and precession minima (insolation maxima), whereas marls deposited during arid phases and precession maxima (insolation minima)

3. Humic phases were typified by high input of degraded terrestrial organic matter driven by enhanced riverine runoff, promoting water column stratification

Primary gypsum with filamentous microfossils

Gypsum with filamentous microfossils from the Piedmont Basin

Dela Pierre et al. 2015

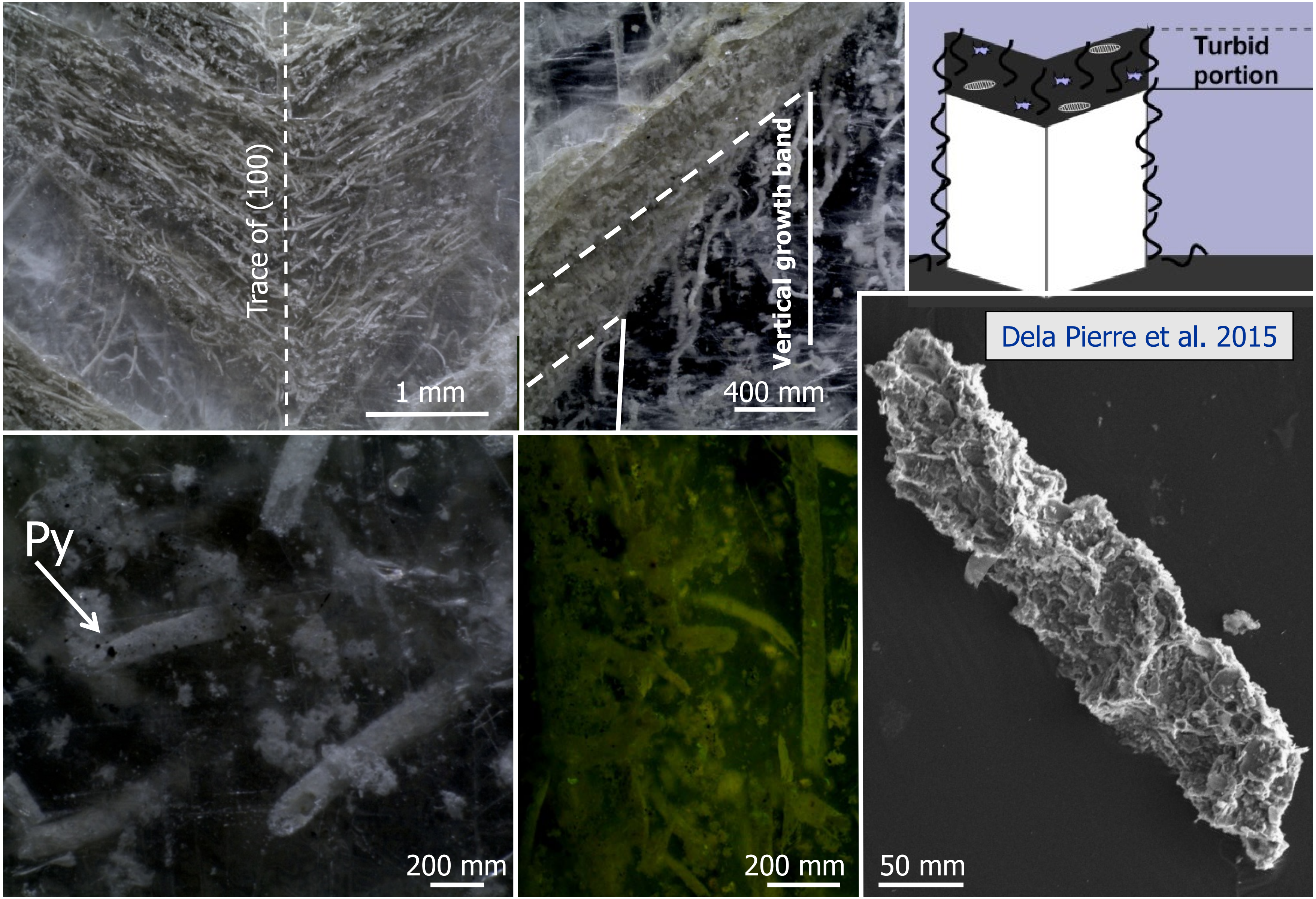
Trace of (100)
1 mm
Vertical growth band
400 mm
Turbid
portion
Dela Pierre et al. 2015
Py
200 mm
200 mm
50 mm

Polysulfide: a clade-diagnostic criterion for sulfide-oxidizing bacteria

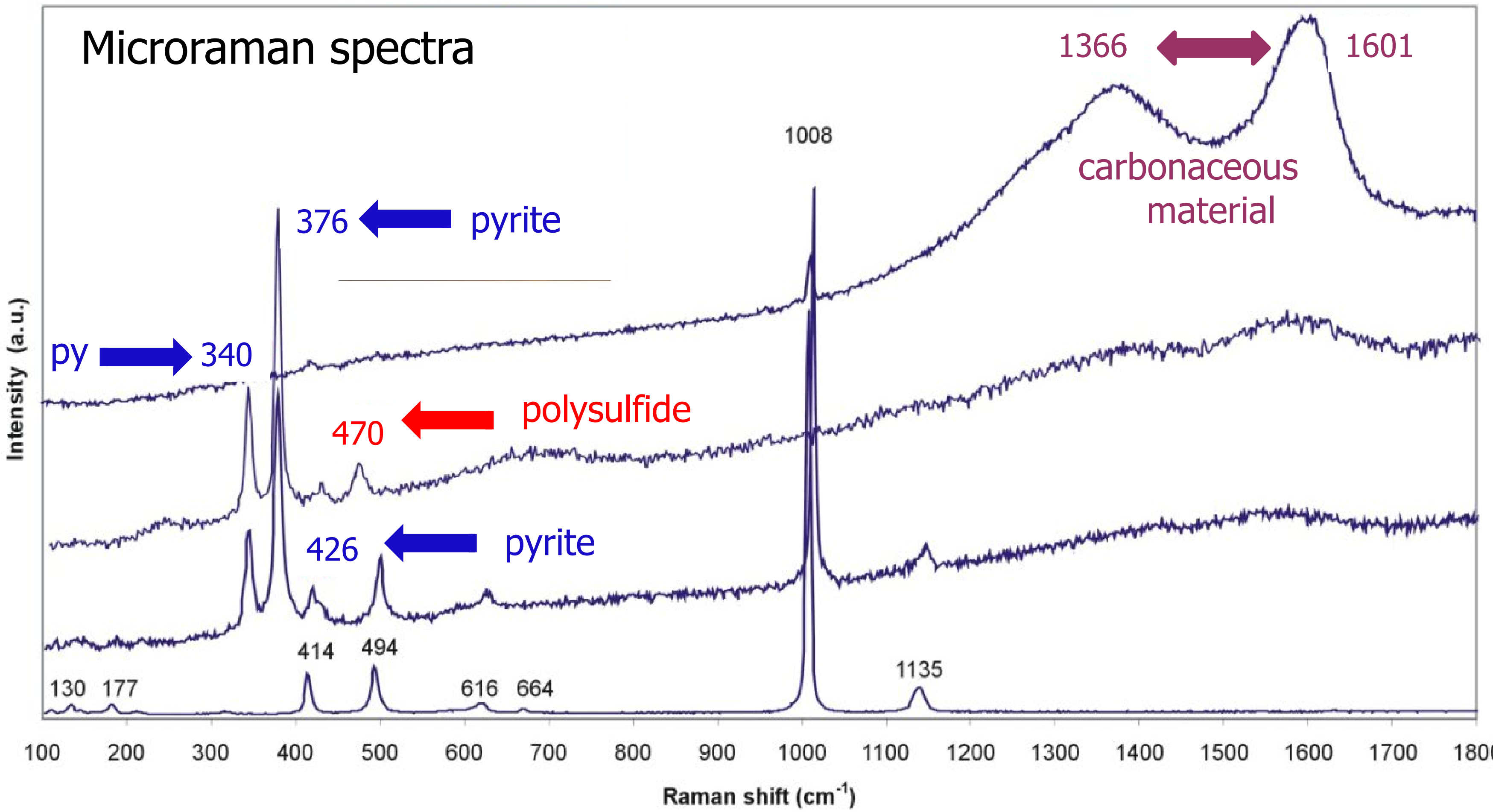

Dela Pierre et al. 2015

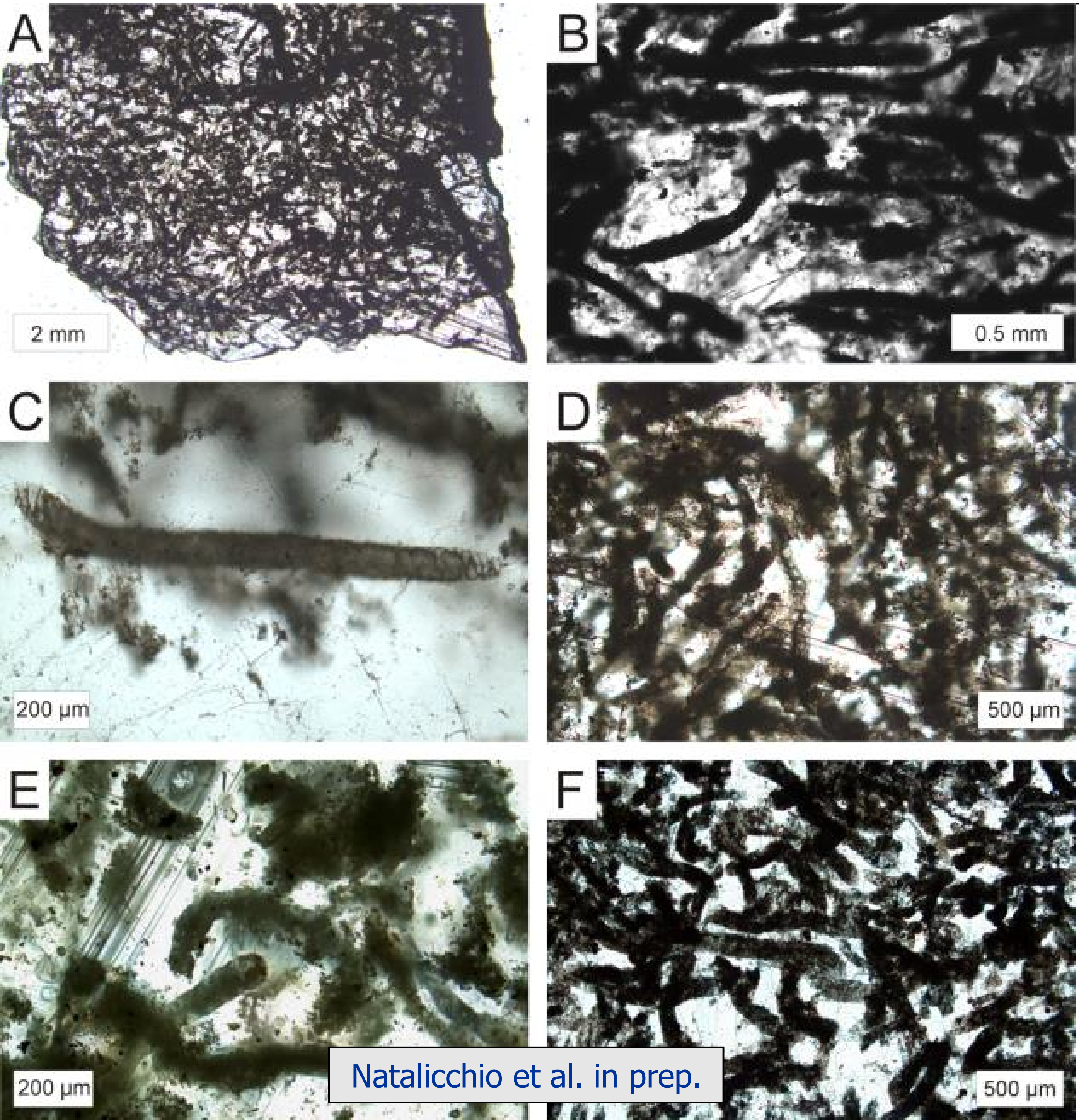

Filamentous microfossils

- algae?
- cyanobacteria?
- sulfide-oxidizing bacteria?

A – Nijar
B – Monte Tondo
C – Monte Tondo
D – Monticinio
E – Crete
F – Cyprus

Diameter of filaments

Panieri et al. 2010: 20 to 30 µm
Schopf et al. 2014: ~70 µm
our data: 60 to 110 µm

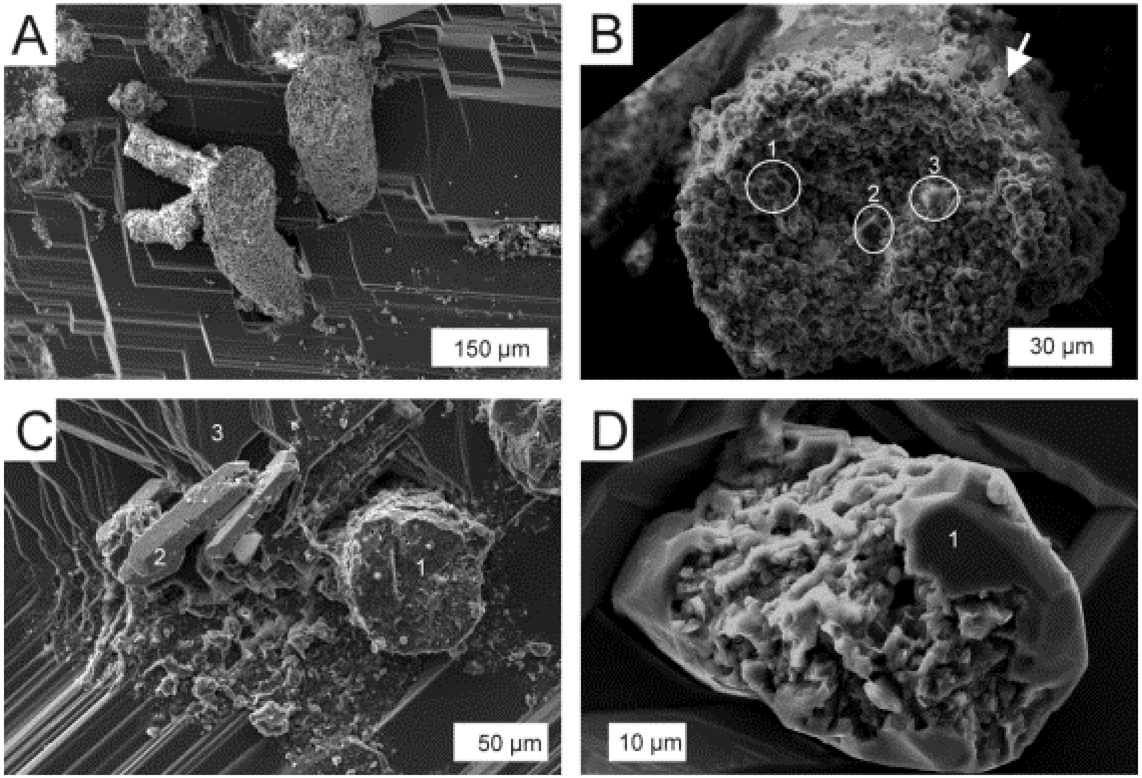

Filamentous microfossils

A – dolomitic filaments, Monte Tondo

B – 1 = dolomite, 2 = celestine,
3 = clay m., Monte Tondo

C – 1 = calcite, 2 = celestine,
3 = gypsum, Monticino

D – 1 = calcite, Monticinio

Natalicchio et al. in prep.

Location	Mineralogy revealed by XRD	additional mineral phases revealed by SEM/EDS
Nijar	gypsum, traces of dolomite	celestine
Monte Tondo	gypsum, traces of dolomite	celestine
Monticino	gypsum	celestine, dolomite, calcite
Crete	gypsum, traces of bassanite	celestine
Cyprus	gypsum	celestine

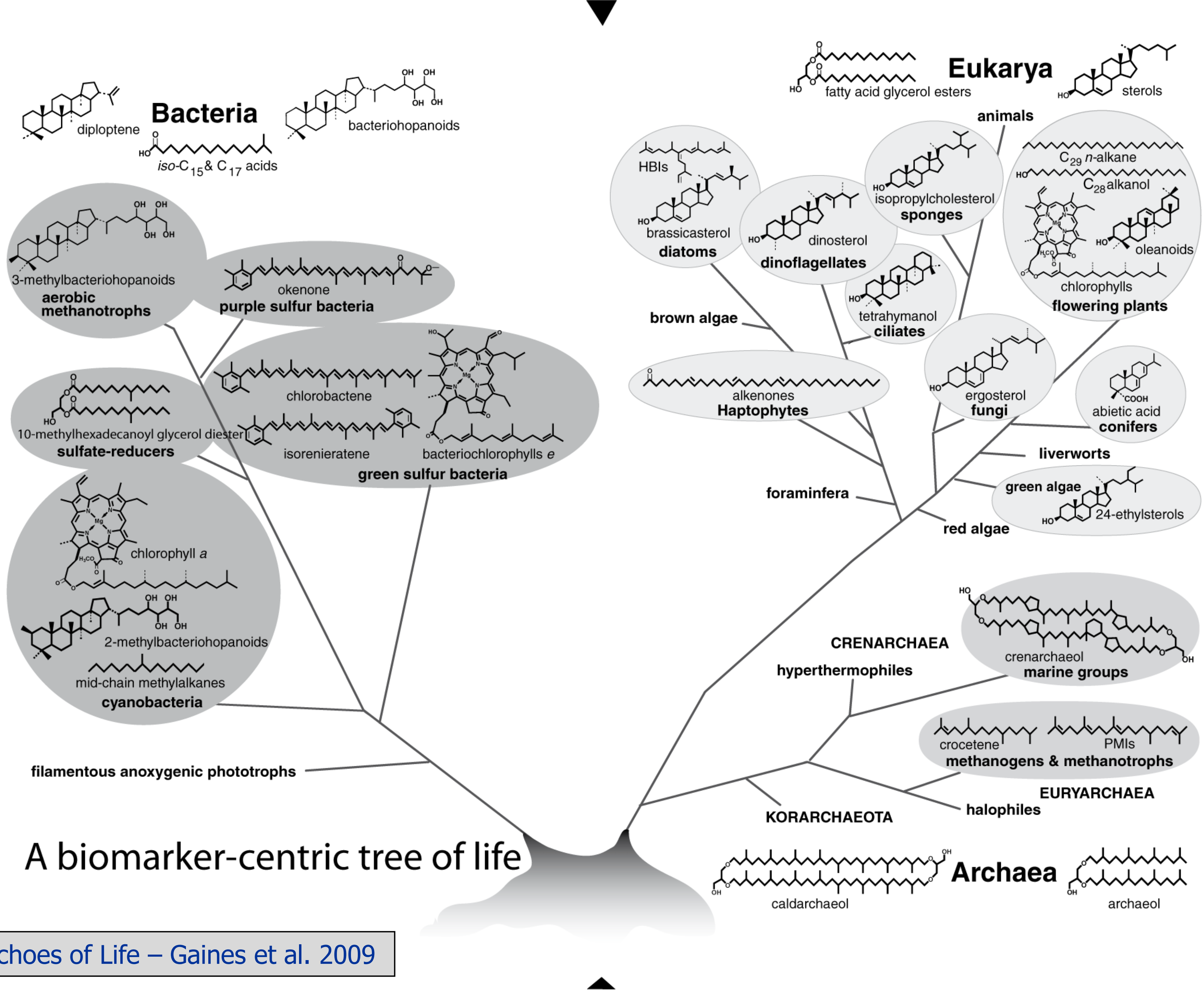

A biomarker-centric tree of life

Echoes of Life – Gaines et al. 2009

Lipid biomarker inventory

	Nijar	Monte Tondo	Monticino	Crete	Cyprus
n-C_{17} / n-C_{18} hydrocarbon ratio	0.7	0.8	0.7	0.8	0.9
Pristane / Phytane ratio	0.7	1.0	0.9	7.3	0.8
TAR_{FA} 1)	0.26	0.50	0.12	0.42	0.43
ACE 2)	93	88	80	98	92
Salinity (‰) 3)	281	267	243	296	279

Natalicchio et al. in prep.

[1] terrestrial/aquatic ratio based on carboxylic acids, $TAR_{FA} = (n\text{-}C_{24}+n\text{-}C_{26}+n\text{-}C_{28})/(n\text{-}C_{14}+n\text{-}C_{16})$

[2] Archaeol Caldarchaeol Ecometric, ACE = (archaeol/(archaeol+caldarchaeol)) *100, <1 = <25 psu, <10 = <50 psu, >40 = >75 psu

[3] calculated after ACE salinity correlation

Conclusions – Filamentous microfossils

1. The biomarker patterns do not allow an unambiguous taxonomic assignment of the filametous microfossils

2. No biomarkers of cyanobacteria have been observed, although the overall preservation of lipids is good

3. The occurrence of polysulfide and pyrite, the diameter of filaments, and the lack of biomarkers of cyanobacteria and algae indicate that the filamentous fossils are colorless sulfide-oxidizing bacteria

Calcare di Base

Universität Hamburg

cen

Biomarker inventory of Calcare di Base from Sicily and Calabria

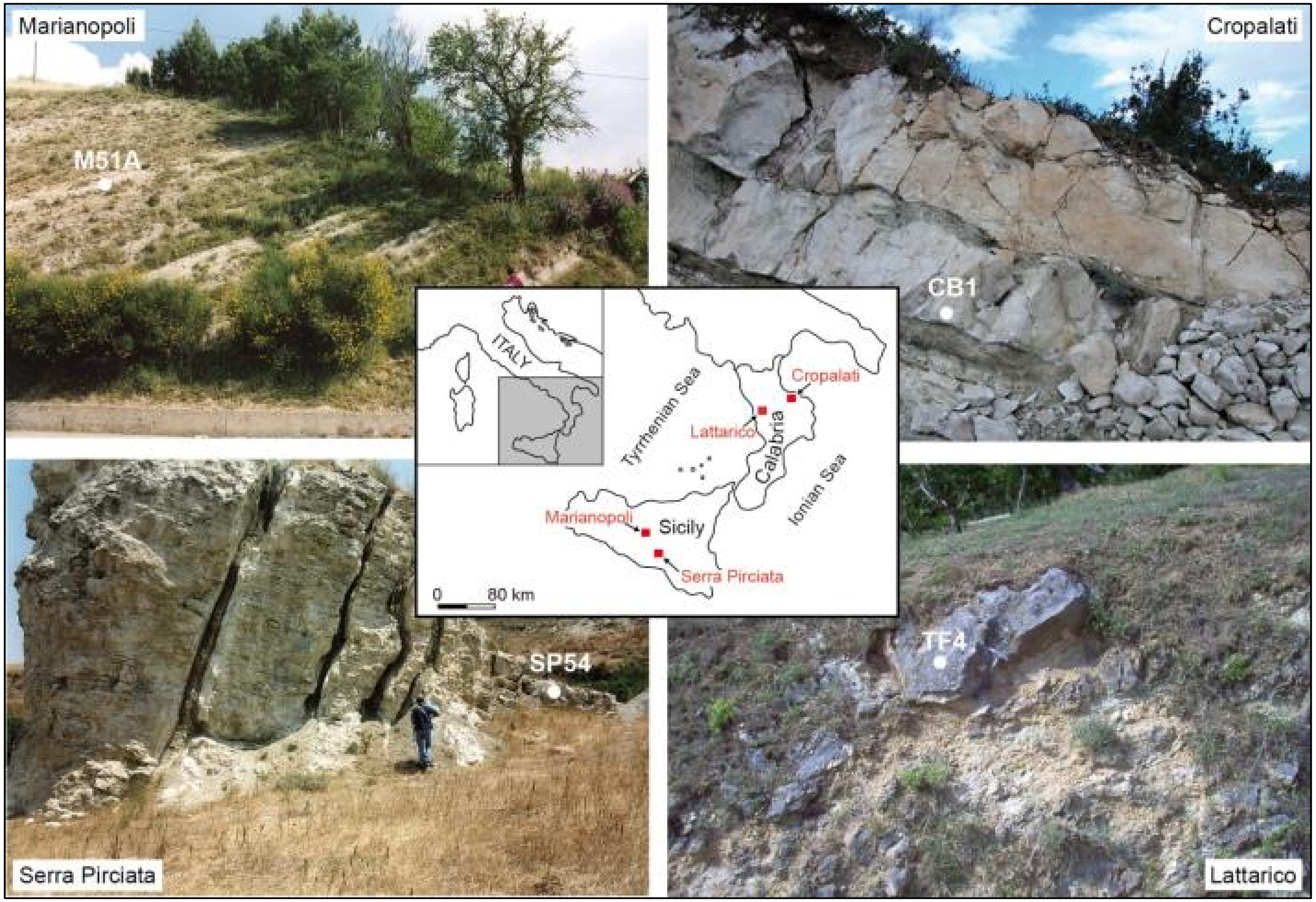

Birgel et al. 2014

Cropalati | Serra Pirciata

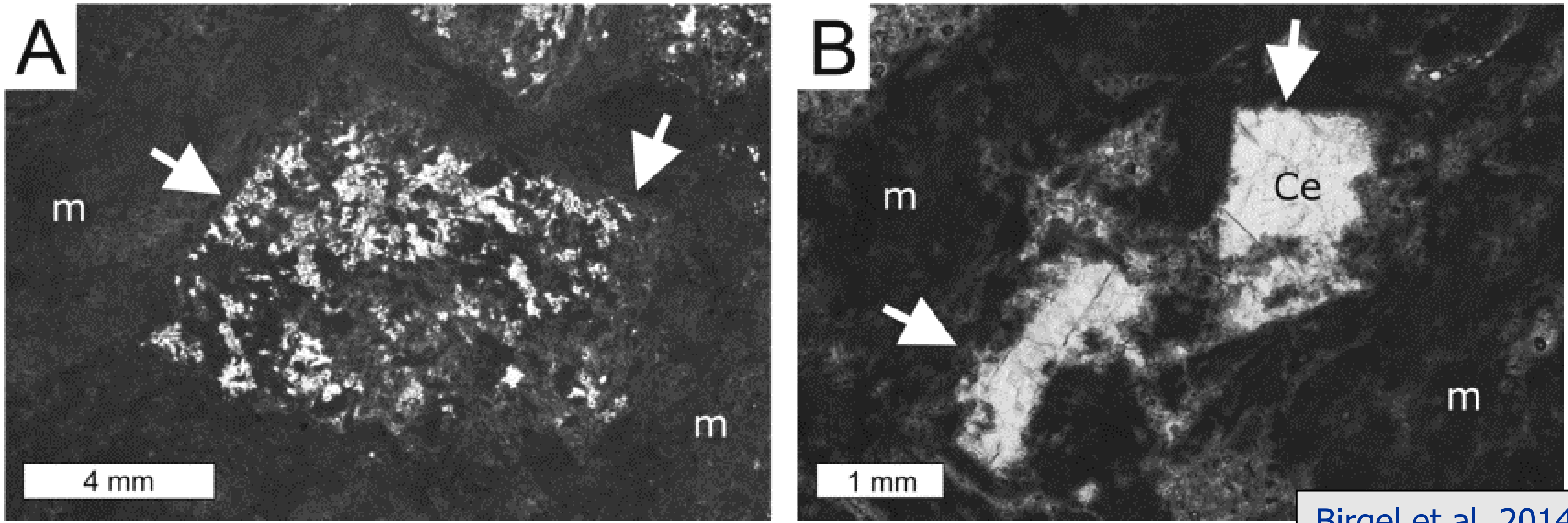

Birgel et al. 2014

m – micrite = microcrystalline calcite

Ce – celestine

Isoprenoid alcohols

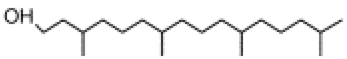

I

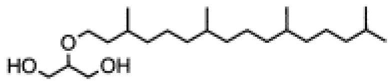

II

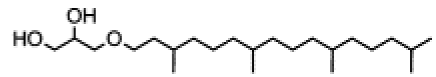

III

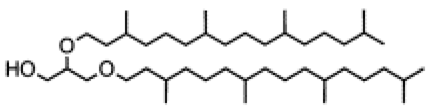

IV

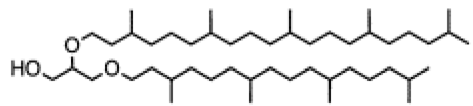

V

I – phytanol

II – *sn*2 phytanyl monoether

III – *sn*3 phytanyl monoether

IV – archaeol

V – extended archaeol

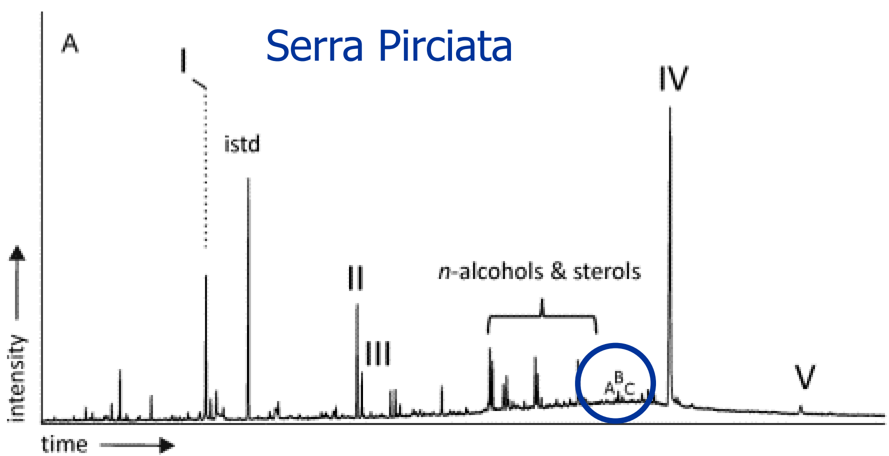

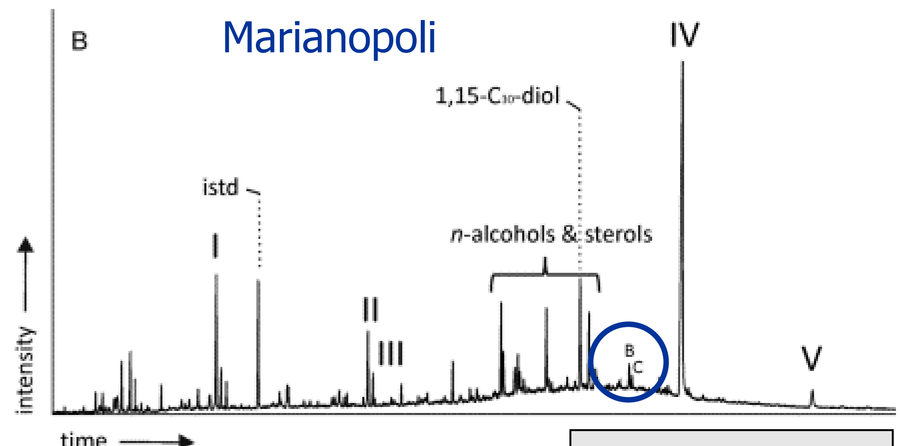

Birgel et al. 2014

Hypersaline conditions revealed by molecular fossils

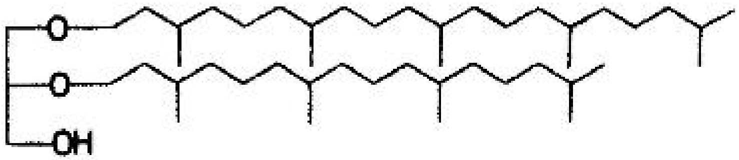

extended archaeol

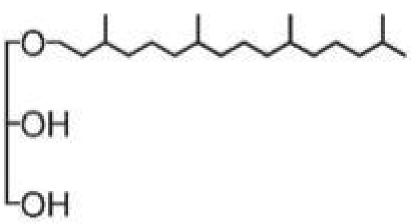

phytanyl monoether

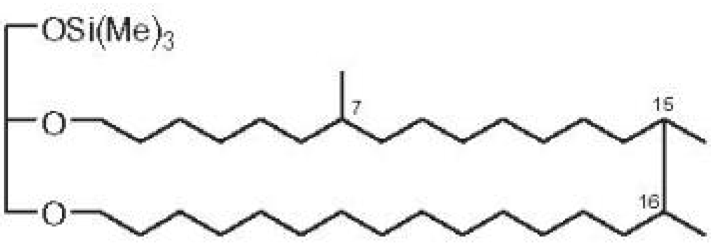

non-isoprenoidal macrocyclic glycerol diether

Proportions of isoprenoid alcohols

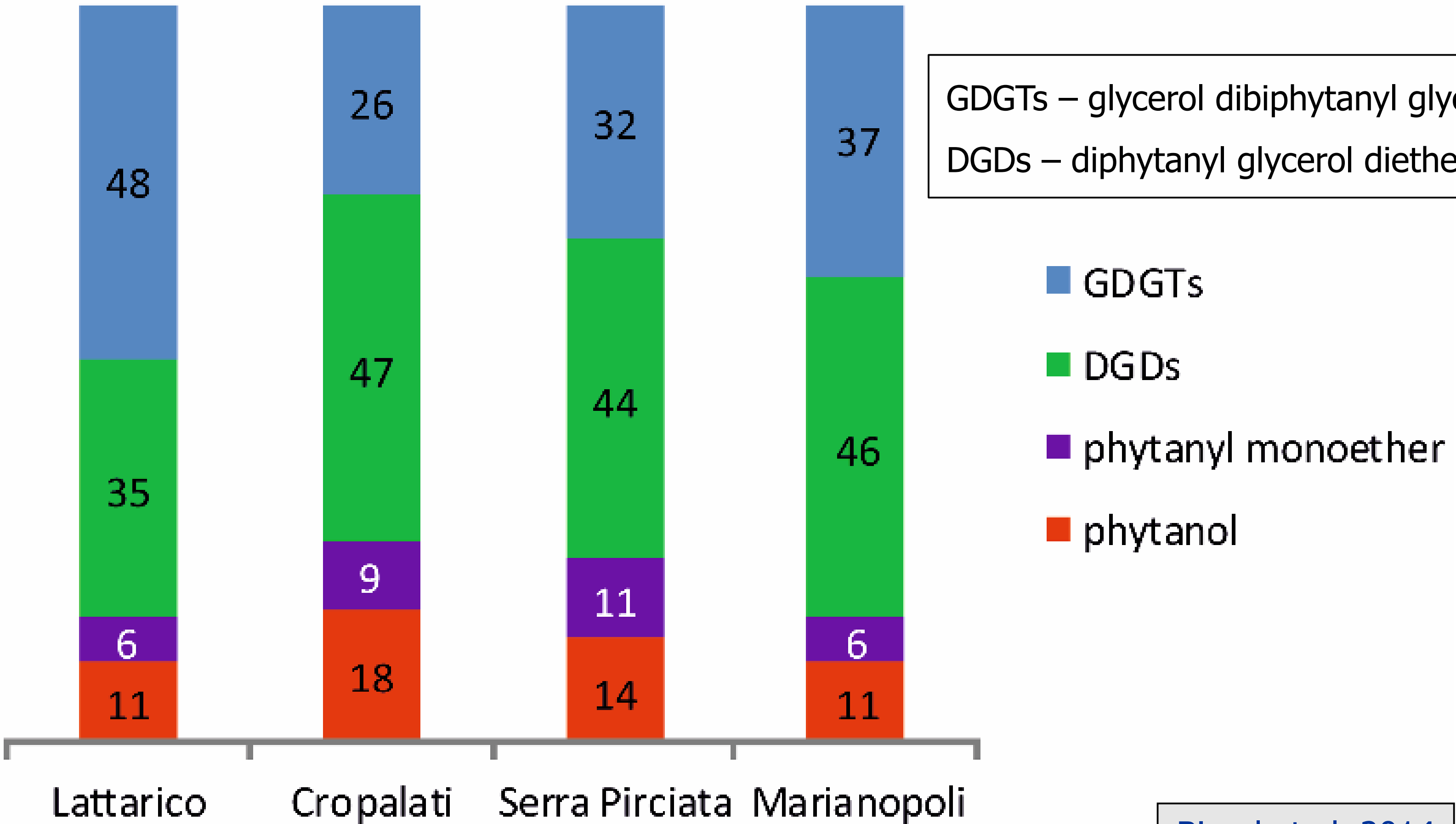

GDGTs – glycerol dibiphytanyl glycerol tetraethers

DGDs – diphytanyl glycerol diethers

Birgel et al. 2014

HPLC-APCI-MS base peak chromatogram

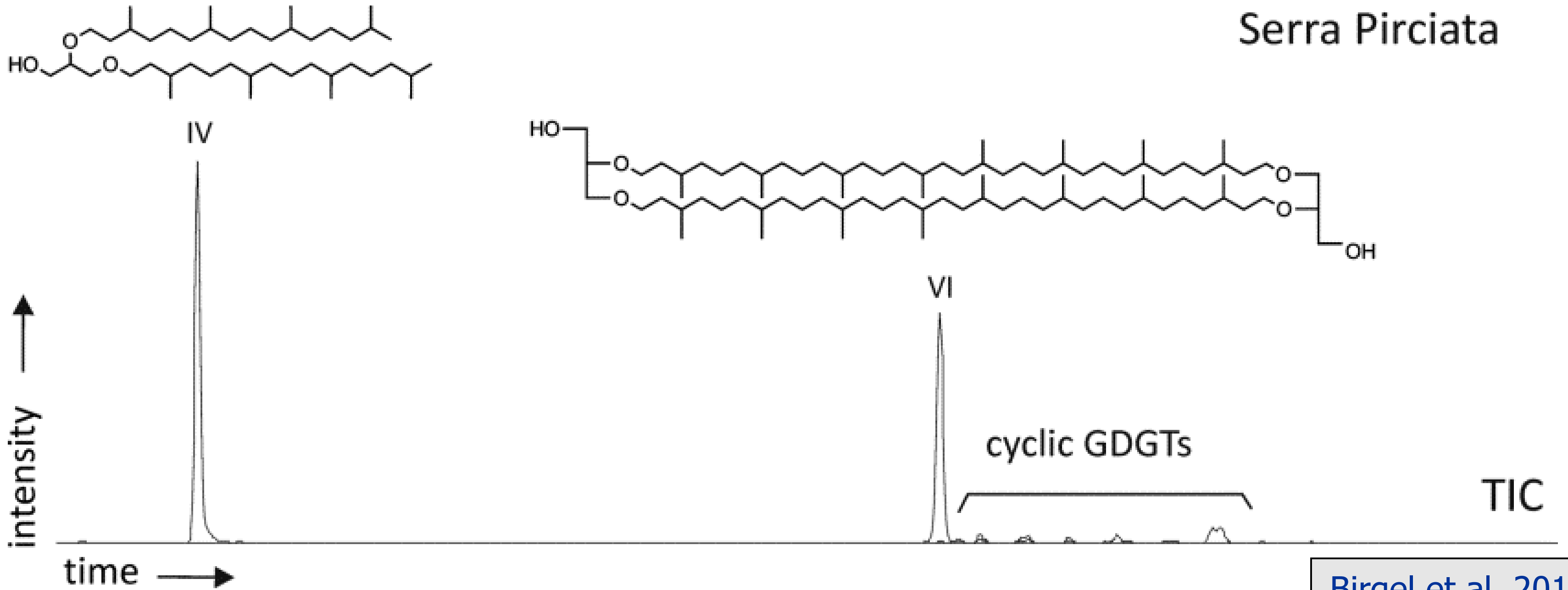

Birgel et al. 2014

Predominance of archaeol (**IV**) over GDGT-0 (**VI**)

Conclusions – Calcare di Base

1. The Calcare di Base formed in hypersaline environments

2. The biomarker inventory is dominated by archaeal lipids; apart from halophilic archaea another group of archaea dwelled in the paleoenvironment, possibly methanogens or members of the Thermoplasmatales

Messinian geomicrobiology team – past and presence

Giovanni Aloisi
Stefano Bernasconi
Daniel Birgel
Benjamin Brunner
Antonio Caruso
Francesco Dela Pierre
Susanne Gier
Adriano Guido
Kai-Uwe Hinrichs
Amanda Labrado
Marcello Natalicchio
Catherine Pierre
Jean-Marie Rouchy
Simon Rouwendaal
Mathia Sabino
Dave Stolwijk
Athina Tzevahirtzian
Simone Ziegenbalg

Funding

Deutsche Forschungsgemeinschaft
European Commission – Marie Slodowska-Curie
Landesgraduierten Hamburg
European Commission – COST action CA15103 MedSalt
European Commission – ETN SALTGIANT

The Messinian Endeavor